Journal of Hazardous Materials 168 (2009) 1134–1139

Contents lists available at ScienceDirect

Journal of Hazardous Materials

journal homepage: www.elsevier.com/locate/jhazmat

Effect of particle size on thermal decomposition of nitrocellulose

M.R. Sovizi [a], S.S. Hajimirsadeghi [a,*], B. Naderizadeh [b]

[a] Faculty of Material and Manufacturing Technologies, Malek Ashtar University of Technology, P.O. Box 16765-3454, Tehran, Iran
[b] Department of Chemistry, Imam Hossein University, Tehran, Iran

ARTICLE INFO

Article history:
Received 2 November 2008
Received in revised form 25 February 2009
Accepted 25 February 2009
Available online 13 March 2009

Keywords:
Nitrocellulose
Nano-fiber
Particle size effect
Thermal decomposition
Non-isothermal

ABSTRACT

Data on the thermal stability of energetic materials such as nitrocellulose were required in order to obtain safety information for handling, storage and usage. In present study, the thermal stability of micron and nano-sized nitrocellulose samples was determined by differential scanning calorimetry (DSC) and simultaneous thermogravimetry–differential thermal analysis (TG/DTA) techniques. The results of TG analysis revealed that the main thermal degradation of nitrocellulose occurs in the temperature range of 190–210 °C. On the other hand, the TG–DTA analysis of samples indicated that particle size of nitrocellulose could affect on its thermal stability and its decomposition temperature decreases by decreasing its particle size. The influence of the heating rate (5, 10, 15 and 20 °C/min) on the DSC behaviour of the nitrocellulose with two particle sizes was verified. The results showed that, as the heating rate was increased, decomposition temperature of the micron and nano-sized compound was increased. Also, the kinetic parameters such as activation energy and frequency factor for the micron and nano-sized nitrocellulose were obtained from the DSC data by non-isothermal methods proposed by ASTM E696 and Ozawa.

1. Introduction

Nitrocellulose is known as a versatile, widely used polymer with numerous applications. For many years, it has been exploited as additive in paints and lacquers, or as an important component for propellant and high explosive formulations [1].

The size of reacting particles affects systems such as propellants, pyrotechnics, and explosives. These reactive systems can involve powders, slurries, or dispersions of a solid or liquid in a gas. In the case of liquids, the droplet size must be taken into consideration. For solids, whether the particles are spherical or jagged, the particle size is important. From a more fundamental point of view, it is the ratio of surface area to mass that must be considered [2]. Much effort has been expended to investigate the effects of particle size for liquid fuels, monopropellants, and explosives. At first glance, the results of these investigations [2] do not seem to be consistent. On the one hand, it is well known [3] that the atomization of a fuel very much reduces its auto-ignition delay. On the other hand, it has also been shown [4] that each fuel, under otherwise identical conditions, has an optimal particle size for a minimum ignition delay: larger particles evidently are not heated sufficiently quickly.

Nano-sized energetic materials have recently become a subject of intense interest. Compared to conventional formulations that use particles with micron diameters with a broad size distribution, nanomaterials offer the possibility of faster energy release, more complete combustion and greater control over performance. A lack of understanding of the fundamental mechanisms has hindered the development of nanoenergetic materials. With conventional particles, chemistry is mainly limited by mass transport [5]. The time for reaction in the diffusion regime is proportional to the square of the particle diameter d^2. As the particle size is reduced, the d^2 behaviour will eventually break down as diffusion-controlled processes and become comparable in rate to chemical reactions [6].

Compatibility studies of different materials by DSC, DTA and TG have been carried out for several years [7–12]. Kinetic studies have become a crucial point in thermal analysis, in which the main purpose is to determine the mechanism of pyrolysis reaction and to calculate the parameters of the Arrhenius equation. These data are required for energetic materials and their related compounds to be qualified for performance and safety in their manufacture, handling, storage and use [13,14].

In this work, the thermal stability of nitrocellulose fibers with various particle size were investigated by means of differential scanning calorimetry (DSC) and simultaneous thermogravimetry–differential thermal analysis (TG–DTA). The results allowed us to acquire information concerning this compound in the solid-state, including its thermal stability and thermal decomposition.

* Corresponding author. Fax: +98 2122936578.
E-mail address: somayyehmirsadeghi@yahoo.com (S.S. Hajimirsadeghi).

0304-3894/$ – see front matter © 2009 Published by Elsevier B.V.
doi:10.1016/j.jhazmat.2009.02.146

Also, this study an attempt has been made to determine the kinetic parameters of non-isothermal decomposition of the micron and nano-sized nitrocellulose. Until today, various data are presented on the thermal behaviour and kinetics of decomposition of micron-sized nitrocellulose compounds [15–24]. Makashir et al. [16] investigated thermal decomposition of nitrocellulose 12.1% nitrate content with regard to kinetics, mechanism, morphology and the gaseous products thereof, using thermogravimetry (TG), differential thermal analysis (DTA), IR spectroscopy, differential scanning calorimetry (DSC) and hot stage microscopy. They investigated kinetics of the initial stage of thermolysis of nitrocellulose in condensed state by isothermal high temperature infrared spectroscopy (IR). Rong et al. [18] were derived two methods for estimating the critical temperature (T_b) of thermal explosion for the highly nitrated nitrocellulose (HNNC) from the Semenov's thermal explosion theory. They obtained values of the thermal decomposition activation energy (E), the onset temperature, the initial temperature and then calculate the critical temperature of thermal explosion for nitrocellulose. In another study, Binke et al. [19] studied melting process of nitrocellulose by using modulated differential scanning calorimetry (MDSC) technique, the microscope carrier method for measuring the melting point and the simultaneous device of the solid reaction cell in situ/RSFT-IR. They obtained values of the melting point, melting enthalpy, melting entropy, the enthalpy of decomposition and the heat-temperature quotient by the MDSC curve of nitrocellulose. Brill and Gongwer [23] analyzed kinetic constants for decomposition of nitrocellulose in the 50–500 °C range. Their results showed that at $T < 100$ °C, three processes (depolymerization, peroxide formation, and hydrolysis) are consistent with the reported kinetics. For $T = 100$–200 °C, 28 of 30 previously reported kinetic measurements can be organized clearly into two categories by the use of the kinetic compensation effect. These two groups fit the first-order and autocatalytic processes. Also, in our previous study, the effect of nitrogen content of nitrocellulose on its thermal decomposition was followed by noting the changes in the TG–DTA and DSC curves [25]. But, to the best of our knowledge, there is no report on the thermal behaviour of nano-sized nitrocellulose.

2. Experimental

2.1. SEM analysis

Particle size of nitrocellulose samples have been tested using a scanning electron microscope. Scanning electron micrographs were recorded by means of a Philips XL30 series instrument using a gold film for loading the dried particles on the instrument. Gold films were prepared by a Sputter Coater model SCD005 made by BAL-TEC (Switzerland).

2.2. Thermal analysis

The nitrocellulose compound with 13.9% nitrate contents in micron particle size was synthesized in our research laboratory (MUT, Tehran) [25]. Also, nitrocellulose nano-fibers were obtained by applying electrospinning to 10 wt% nitrocellulose solutions in ethyl methyl keton (EMK) [26].

Thermochemical behaviour of nitrocellulose samples with different particle size (micron and nano-sized) was characterized. The DSC curves were obtained by Du Pont differential scanning calorimeter model DSC 910S, in temperature rang of 50–400 °C using an open aluminum crucible, at different heating rates (5, 10, 15 and 20 °C/min), under helium atmosphere with the flow rate of 50 ml min^{-1}. The sample mass used for DSC experiments was about 3.0 mg.

Simultaneous thermogravimetric analysis (TG) and differential thermal analysis (DTA) were carried out using a Stanton Redcroft, STA-780 series with an open alumina crucible, applying heating rate of 10 °C/min in a temperature range of 50–400 °C, under helium atmosphere with the flow rate of 50 ml min^{-1}. The sample mass used was about 3.0 mg.

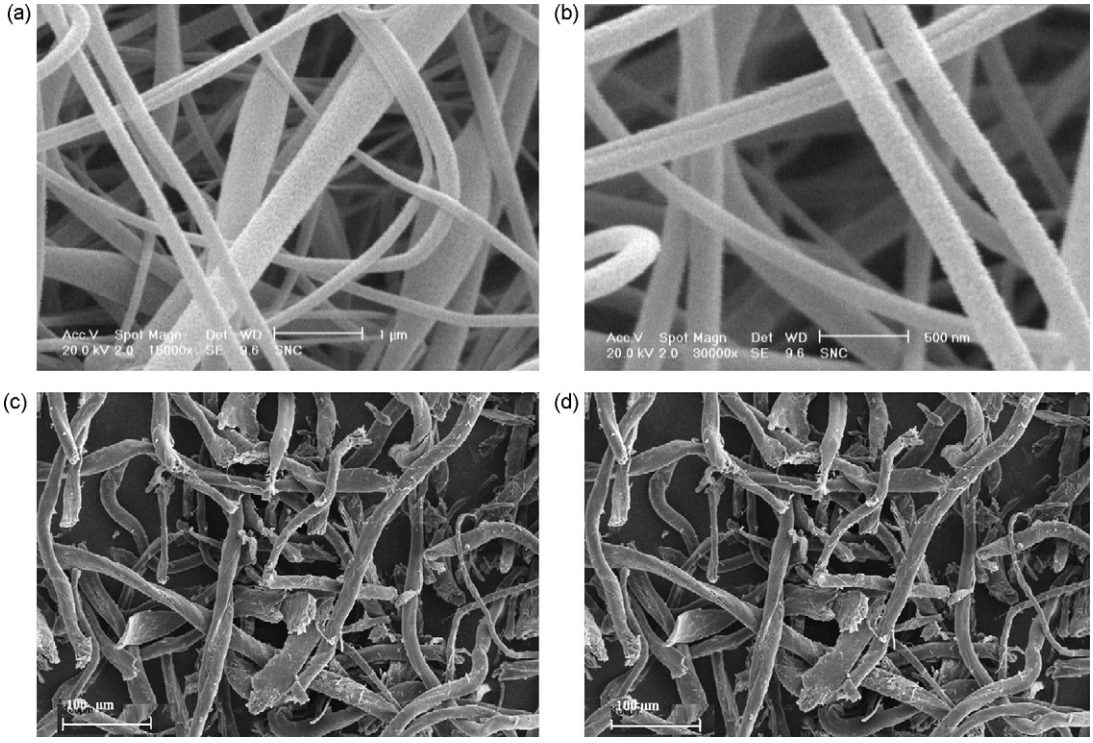

Fig. 1. SEM images of fibrous nitrocellulose: (a and b) nano-fibers and (c and d) micron-sized fibers.

Table 1
Summary of experimental results for DTA/TG of micron and nano-sized nitrocellulose.

No.	Sample	Transition temperature[a] (°C)		
		Onset	Maximum	T[b]
1	Micron-sized	198.2 (±0.1)	208.1	198–210
2	Nano-sized	190.8 (±0.2)	202.8	190–205

[a] These temperatures are peak temperatures at maximum heat flux.
[b] *T* is the temperature range associated with a variation sample's mass (decrease).

3. Results and discussion

3.1. Results of SEM analysis

Fig. 1 shows SEM photographs of different samples of nitrocellulose, nano-fiber sample (Fig. 1a and b) and microfibers sample (Fig. 1c and d). It is clear that two different morphologies could be detected among the generated nano-fibers. The surface of the nano-fibers with 90–150 nm diameters appears smooth while some pores are observed on the surface of the fibers with greater diameters range from 400 to 500 nm.

On the other hand, the results of SEM confirmed the well-known fibrous structure of NC which the microfibers have 20–30 μm average size in diameter without any agglomeration.

3.2. Results of thermal analysis

The thermoanalytical results of micron-sized nitrocellulose are presented in Table 1. The TG/DTA curves showed a single sharp exothermic behaviour with a maximum at 208.1 °C, accompanied by a sharp weight loss. Previous studies [27] showed that, the decomposition of micron-sized nitrocellulose at this temperature produces H_2O, CO, NO and CO_2 as evolved gases and CO is the major decomposition product of nitrocellulose. Also, thermomicroscopy showed [28] that the nitrocellulose melted in the region of 200 °C to give a highly mobile bubbling liquid. There was no indication of melting on the DTA curve, presumably because any endothermic effect was out-weighted by the concurrent exothermic decomposition.

On the other hand, for the nitrocellulose nano-fibers, a thermal pattern quite similar to its micron sized was obtained. The DTA and TG curves of nano-sized nitrocellulose are shown in Fig. 2. But, the results showed that thermal stability of nitrocellulose decreases with decreasing its particle size from micron to nano-sized and the nitrocellulose nano-fibers decompose at ~190.8 °C with decrease in the weight of sample in temperature range of 190–205 °C. For this particle size, onset decomposition temperature (190.2 °C) is lower than the decomposition point of the micron sized (198 °C, see Table 1).

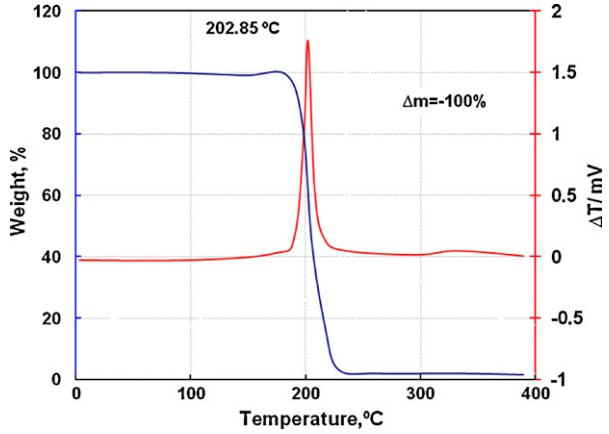

Fig. 2. TG/DTA curves for nitrocellulose nano-fibers; sample mass 3.0 mg; heating rate 10 °C/min; helium atmosphere.

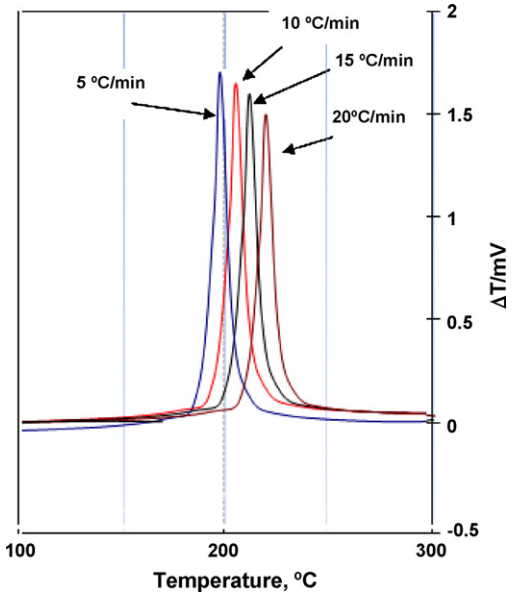

Fig. 3. Effect of heating rate on the nitrocellulose nano-fibers DSC results; sample mass 3.0 mg; helium atmosphere with the flow rate of 50 ml min^{-1}.

3.3. Effect of heating rate

Fig. 3 shows DSC curves of the nano-fibers of nitrocellulose at several heating rates. It was found that, by increasing the heating rate, the decomposition temperature of the nitrocellulose was shifted to higher temperatures. These shifts in onset temperature and peak temperature are shown in Table 2. Also, the results of this study show that as the particle size of nitrocellulose was increased, the enthalpy of decomposition obtained by area under DSC peaks was increased. These changes in enthalpy of decomposition are shown in Fig. 4.

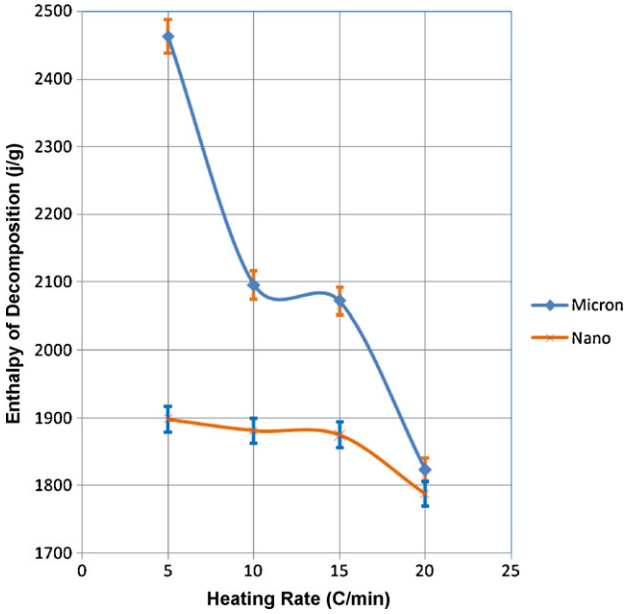

Fig. 4. The effect of various heating rate on enthalpy of decomposition (obtained from area under DSC peaks) for nitrocellulose samples.

Table 2
Onset and maximum decomposition temperature of nitrocellulose samples with various particle sizes obtained by DSC at various heating rate.

Heat flow (°C/min)	Particle size			
	Nano-size		Micron-size	
	Onset temperature (°C)	Maximum temperature (°C)	Onset temperature (°C)	Maximum temperature (°C)
5	178.7 (±0.1)	190.2	192.2 (±0.2)	201.8
10	190.8 (±0.1)	202.8	198.2 (±0.1)	208.1
15	193.5 (±0.2)	207.3	202.1 (±0.1)	213.6
20	202.2 (±0.2)	214.3	205.1 (±0.1)	218.0

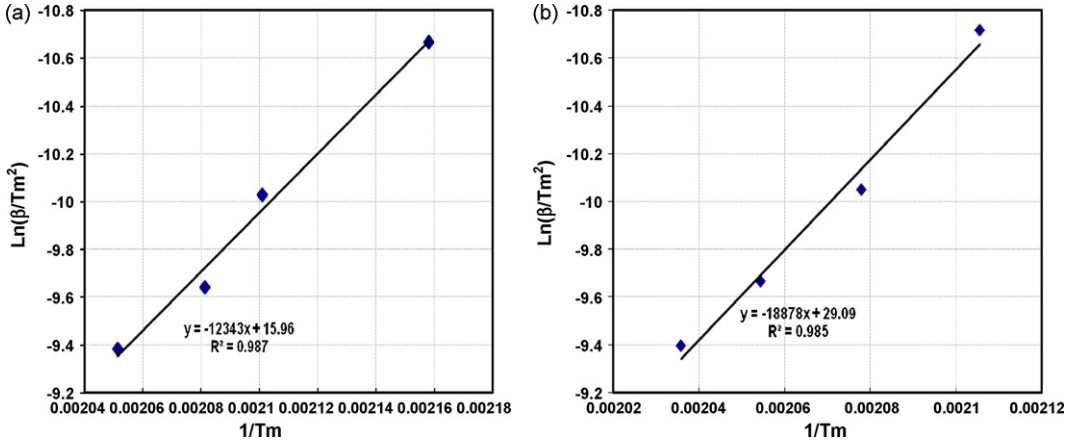

Fig. 5. Plot of $ln(\beta T_{m-2})$ versus reciprocal peak temperature $1/T_m$ for nitrocellulose samples with (a) nano- and (b) micron-size. The data derived from DSC experiments in helium atmosphere.

3.4. Kinetic methods

The ASTM method E698 [29] was used to determine the Arrhenius parameters for the thermal decomposition of two studied nitrocellulose particle size. In order to calculate the pre-exponential factor (Z), it was assumed that the decomposition followed first-order kinetics. The DSC curves obtained at various heating rates for nano-sized nitrocellulose are shown in Fig. 3. The values of T_m were corrected for scale non-linearity, heating rate changes, and thermal lag as described in the ASTM E 698-05 standard.

The plot of the $\ln(\beta T_{m-2})$ against $1/T_m$ was straight lines for nitrocellulose with various particle sizes (Fig. 5). Thus, first-order kinetics provides a good description of the overall observed decomposition behaviour in this temperature range [30]. The slope of the lines was equal to $-E_a/R$. Therefore, the activation energy (E_a) was obtained from the slope of the graph while the log of the pre-exponential factor, $\log(Z/S^{-1})$ was calculated from the expression given in ASTM E698:

$$Z = \beta \left(\frac{E_a}{RT_{m^2}}\right) exp\left(\frac{E_a}{RT_m}\right) \quad (1)$$

Table 3 contains the calculated values of activation energy and frequency factors for nitrocellulose samples. On the other and, activation energy (E_a) for both samples was calculated by Ozawa method. In this method, activation energy could be determined from plots of the logarithm of the heating rate versus the inverse of the temperature at the maximum reaction rate in constant heating rate experiments. The activation energy can be determined by Ozawa method without a precise knowledge of the reaction mechanism, using the following equation:

$$\log \beta + 0.496 \frac{E_a}{RT_m} = C \quad (2)$$

The activation energy of decomposition of the studied nitrocellulose samples was estimated using Ozawa method. The plot of logarithm of heating rates versus reciprocal of the absolute peak temperature for the micron and nano-sized samples was straight lines with $r = 0.9933$ and $r = 0.9948$, respectively, which indicated that the mechanism of thermal decomposition of nitrocellulose over this temperature range did not vary [31]. On the other hand, frequency factor (Z) was found for the compound from Eq. (1).

All resulted data are summarized in Table 3. Comparing the results of the application of the two methods, we observe that values calculated for nitrocellulose samples by ASTM and Ozawa methods are comparable.

After the kinetic parameters (E and A) were obtained, the thermodynamic parameters of activation can be calculated from the following equations [32,33]:

$$A \ \exp \frac{-E}{RT} = \nu \exp \frac{-\Delta G^{\#}}{RT} \quad (3)$$

Table 3
Comparison of kinetic parameters of the nitrocellulose samples obtained by ASTM and Ozawa methods.

Particle size	Method	Activation energy (kJ/mol)	Frequency factor $\log Z\ (S^{-1})$	Linear regression (r)	$\Delta G^{\#}$ (kJ/mol)	$\Delta H^{\#}$ (kJ/mol)	$\Delta S^{\#}$ (J/mol)	$-\log K$
Nano	ASTM	102.5 (±0.3)	11.01 (±0.03)	0.9940	120.55	98.55	−46	6.99
	Ozawa	105.15 (±0.3)	11.31 (±0.04)	0.9948	120.43	101.19	−40	7.33
Micron	ASTM	157.2 (±0.1)	16.98 (±0.03)	0.9926	121.20	153.29	68	10.59
	Ozawa	157.4 (±0.4)	16.96 (±0.05)	0.9933	121.57	153.48	68	10.64

r = linear regression coefficient; $\Delta G^{\#}$, $\Delta H^{\#}$ and $\Delta S^{\#}$ are given at decomposition temperature of nano-fibers nitrocellulose that is 202.8 °C.

$$\Delta H^{\#} = E - RT \quad (4)$$

$$\Delta G^{\#} = \Delta H^{\#} - T\Delta S^{\#} \quad (5)$$

where $\Delta G^{\#}$, $\Delta H^{\#}$ and $\Delta S^{\#}$ are free energy, enthalpy and entropy of the activation, receptivity. υ is the $\upsilon = K_B T/h$ (where K_B and h are Boltzmann and Plank constant, respectively). Table 3 gives the computed thermodynamic parameters for micron and nano-sized nitrocellulose samples.

3.5. Decomposition reaction rate constant

Assuming a first-order decomposition, the equation to determine the half-life would be: $t_{1/2} = 0.693/k$. The rate constant (k) for decomposition reaction could be calculated by the following equation [31]:

$$\log k = \log A - \frac{E_a}{2.3RT} \quad (6)$$

From above equation rate constant (k) was calculated at 25 °C. Table 3 listed the rate constant for these decomposition reaction.

3.6. Critical explosion temperature

The critical explosion temperature (T_b) is an important parameter required to insure safe storage and process operations involving explosives, propellants and pyrotechnics. It is defined as the lowest temperature to which a specific charge may be heated without undergoing thermal runaway [34–36]. T_b may be calculated from inflammation theory and appropriate thermokinetic parameters namely the activation energy, pre-exponential factor, and heat of reaction. In order to obtain the critical temperature of thermal explosion (T_b) for the nitrocellulose samples, Eqs. (7) and (8) were used [37].

$$T_e = T_{e0} + b\phi_i + c\phi_i^2, \quad i = 1 - 4 \quad (7)$$

$$T_b = \frac{E - \sqrt{E^2 - 4ERT_{e0}}}{2R} \quad (8)$$

where b and c are coefficients, R is the gas constant; E is the value of activation energy obtained by kinetic method.

The value (T_{e0}) of the onset temperature (T_e) corresponding to $\phi \to 0$ obtained by Eq. (7) is 185.3 °C and 168.9 °C for micron and nano-sized nitrocellulose, respectively.

The critical temperature of thermal explosion (T_b) obtained from Eq. (8) is 196.7 °C and 186.0 °C for micron and nano-sized nitrocellulose by using ASTM and Ozawa data, respectively.

3.7. Comparison of decomposition temperatures of micro and nano samples

In this study, the thermal behaviour of two nitrocellulose samples with different particle sizes was studied in identical conditions. For the nano-sized nitrocellulose, as seen in Fig. 2 and Table 1, decomposition occurred at 202.8 °C with a fall in the weight of sample. Also, for micron-sized sample, the decomposition was happened about 208 °C. On the other hand, as the results show, the decomposition temperatures of two samples were different and micron-sized sample shows higher decomposition temperatures about 6 °C in comparison with nano-sized sample. A comparison of decomposition temperature of these samples is shown in Table 1.

The values of the kinetic parameters that were obtained by the ASTM and Ozawa methods for micron and nano-sized samples showed good correlation, but the values of activation energy obtained by Ozawa method for micron and nano-sized nitrocellulose fibers were slightly higher than those obtained by ASTM method. On the other hand, the values of $\Delta S^{\#}$, $\Delta G^{\#}$ and $\Delta H^{\#}$ of the decomposition reaction of both nitrocellulose samples were computed. Our finding showed that, the values of the $\Delta G^{\#}$ for the decomposition of micron-sized sample is higher than decomposition of nano-sized nitrocellulose. Also, the values of the activation enthalpies ($\Delta H^{\#}$) and activation energy have the same trends. Thus, thermal stability of the nitrocellulose samples obeys the following order: micron-sized > nano-sized.

4. Conclusion

This study indicates that thermal decomposition of nitrocellulose occurs in a single step. Also, the results showed that first-order process best describes the DSC plots for both micron and nano-sized nitrocellulose in the investigated temperature range. Kinetic parameters were deduced for single decomposition step under non-isothermal condition. The kinetic parameters obtained from ASTM method are in good agreement with those of the Ozawa method. It was found that thermal stability of both samples increased as the heating rate increased. Additionally, all thermal stability and kinetic parameters for the micron-sized nitrocellulose is higher than that obtained for the nano-sized nitrocellulose. Thus, nano-sized nitrocellulose fibers could be used for applications, which require more sensitivity. Based on the kinetic data obtained for the activation energy by ASTM and Ozawa methods, using non-isothermal thermal analysis experiments, the ratio of activation energy for micron to nano-sized nitrocellulose is approximately 1.5. These results show that nano-sized nitrocellulose in comparison with micron-sized nitrocellulose is a heat sensitive and needs more care during storage period.

References

[1] M.A. Hassan, Effect of malonyl malonanilide dimers on the thermal stability of nitrocellulose, J. Hazard. Mater. A88 (2001) 33–49.
[2] M. Fathollahi, S.M. Pourmortazavi, S.G. Hosseini, The effect of the particle size of potassium chlorate in pyrotechnic compositions, Combust. Flame 138 (2004) 304–306.
[3] B. Berger, A.J. Brammer, E.L. Charsley, J.J. Rooney, S.B. Warrington, Thermal analysis studies on the boron–potassium perchlorate–nitrocellulose pyrotechnic system, J. Therm. Anal. Calorim. 49 (1997) 1327–1355.
[4] J.H. Mclain, Pyrotechnic from the Viewpoint of Solid State Chemistry, Franklin Institute Press, 1980, pp. 26–37.
[5] E.W. Price, Combustion of metalized propellants, in: K. Kuo, M. Summerfield (Eds.), Fundamentals of Solid-Propellant Combustion, Progress in Aeronautics and Astronautics, vol. 90, AIAA, New York, 1984, pp. 479–485.
[6] Y. Yanqiang, S. Zhaoyong, W. Shufeng, D.D. Dana, Fast spectroscopy of laser-initiated nanoenergetic materials, J. Phys. Chem. B 107 (2003) 4485–4493.
[7] A. Eslami, S.G. Hosseini, S.M. Pourmortazavi, Thermoanalytical investigation on some boron-fuelled binary pyrotechnic systems, Fuel 87 (2008) 3339–3343.
[8] S.G. Hosseini, S.M. Pourmortazavi, S.S. Hajimirsadeghi, Thermal decomposition of pyrotechnic mixtures containing sucrose with either potassium chlorate or potassium perchlorate, Combust. Flame 141 (2005) 322–326.
[9] L.A. Ramos, E.T.G. Cavalheriro, G.O. Chierice, Preparation, characterization and thermal decomposition of ammonium salts of dithiocarbamic acids, J. Therm. Anal. Calorim. 79 (2005) 349–353.
[10] G. Singh, C.P. Singh, S.M. Mannan, Thermolysis of some transition metal nitrate complexes with 1,4-diamino butane ligand, J. Hazard. Mater. B122 (2005) 111–117.
[11] S.M. Pourmortazavi, S.S. Hajimirsadeghi, S.G. Hosseini, Characterization of the aluminum/potassium chlorate mixtures by simultaneous thermogravimetry–differential thermal analysis, J. Therm. Anal. Calorim. 84 (2006) 557–561.
[12] G. Singh, R. Prajapati, R. Frohlich, Studies on energetic compounds Part 45. Synthesis and crystal structure of disodium azotetrazole pentahydrate, J. Hazard. Mater. A118 (2005) 75–78.
[13] I.P.S. Kapoor, P. Srivastava, G. Singh, Preparation, characterization and thermolysis of phenylenediammonium dinitrate salts, J. Hazard. Mater. 150 (2008) 687–694.
[14] S.M. Pourmortazavi, M. Fathollahi, S.S. Hajimirsadeghi, S.G. Hosseini, Thermal behavior of aluminum powder and potassium perchlorate mixtures by DTA and TG, Thermochim. Acta 443 (2006) 129–131.
[15] A. Książczak, T. Gołofit, W. Tomaszewski, Binary system nitrocellulose from linters+ *sym*–diethyldiphenylurea, J. Therm. Anal. Calorim. 91 (2008) 375–380.
[16] P.S. Makashir, R.R. Mahajan, J.P. Agrawal, Studies on kinetics and mechanism of initial thermal decomposition of nitrocellulose, J. Therm. Anal. Calorim. 45 (1995) 501–509.

[17] A. Książczak, T. Książczak, M. Ostrowski, Intermolecular interactions and phase equilibria in nitrocellulose—*s*-diethyldiphenylurea system, J. Therm. Anal. Calorim. 74 (2003) 575–581.
[18] L. Rong, N. Binke, W. Yuan, Y. Zhengquan, H. Rongzu, Estimation of the critical temperature of thermal explosion for the highly nitrated nitrocellulose using non-isothermal DSC, J. Therm. Anal. Calorim. 58 (1999) 369–373.
[19] N. Binke, L. Rong, C. Xianqi, W. Yuan, H. Rongzu, Y. Qingsen, Study on the melting process of nitrocellulose by thermal analysis method, J. Therm. Anal. Calorim. 58 (1999) 249–252.
[20] A. Książczak, A. Radomski, T. Zielenkiewicz, Nitrocellulose porosity–thermoporometry, J. Therm. Anal. Calorim. 74 (2003) 559–568.
[21] G. Herder, W.P.C. de Klerk, Measurement of the relaxation transitions of nitrocellulose based gunpowder, J. Therm. Anal. Calorim. 85 (2006) 169–173.
[22] M.A. Bohn, Kinetic modeling of the concentrations of the stabilizer DPA and some of its consecutive products as function of time and temperature, J. Therm. Anal. Calorim. 65 (2001) 103–120.
[23] T.B. Brill, P.E. Gongwer, Thermal decomposition of energetic materials 69. Analysis of the kinetics of nitrocellulose at 50–500 °C, Propel. Expl. Pyrotech. 22 (2004) 38–44.
[24] M.A. Hassan, A.B. Shehata, Studies on some acrylamido polymers and copolymer as stabilizers for nitrocellulose, J. Appl. Polym. Sci. 85 (2002) 2808–2819.
[25] S.M. Pourmortazavi, S.G. Hosseini, M. Rahimi-Nasrabadi, S.S. Hajimirsadeghi, H. Momenian, Effect of nitrate content on thermal decomposition of nitrocellulose, J. Hazard. Mater. 162 (2009) 1141–1144.
[26] M.M. Demir, I. Yilgor, E. Yilgor, B. Erman, Electrospinning of polyurethane fibers, Polymer 43 (2002) 3303–3309.
[27] L. Huwei, F. Ruonong, Studies on thermal decomposition of nitrocellulose by pyrolysis-gas chromatography, J. Anal. Pyrol. 14 (1988) 163–167.
[28] B. Berger, E.L. Charsley, S.B. Warrington, Characterization of the zirconium/potassium perchlorate/nitrocellulose pyrotechnic system by simultaneous thermogravimetry–differential thermal analysis–mass spectrometry, Propel. Expl. Pyrotech. 20 (1995) 266–272.
[29] ASTM E 698-05, Standard test methods for Arrhenius kinetic constants for thermally unstable materials using differential scanning calorimetry and the Flynn/Wall/Ozawa method.
[30] M. Sunitha, C.P. Reghunadhan Nair, K. Krishnan, K.N. Ninan, Kinetics of Alder-ene reaction of tris(2-allylphenoxy)triphenoxycyclotriphosphazene and bismaleimides; a DSC study, Thermochim. Acta 374 (2001) 159–169.
[31] A.S. Tompa, R.F. Boswell, Thermal stability of a plastic bonded explosive, Thermochim. Acta 357–358 (2000) 169–175.
[32] J.M. Criado, L.A. Perez-Maqueda, P.E. Sanchez-Jimenez, Dependence of the pre-exponential factor on temperature, J. Therm. Anal. Calorim. 82 (2005) 671–675.
[33] M.O. Humienik, J. Mozejko, Thermodynamic functions of activated complexes created in thermal decomposition processes of sulphates, Thermochim. Acta 344 (2000) 73–79.
[34] J.M. Pickard, Critical ignition temperature, Thermochim. Acta 392 (2002) 37–40.
[35] A.K. Burnham, R.K. Weese, A.P. Wemhoff, J.L. Maienschein, A historical and current perspective on predicting thermal cook-off behavior, J. Therm. Anal. Calorim. 89 (2007) 407–415.
[36] M. Sućeska, A computer program based on finite difference method for studying thermal initiation of explosives, J. Therm. Anal. Calorim. 68 (2004) 865–875.
[37] T.L. Zhang, R.Z. Hu, Y. Xie, F.P. Li, The estimation of critical temperatures of thermal explosion for energetic materials using non-isothermal DSC, Thermochim. Acta 244 (1994) 171–176.